

# Chapter 1

## Introduction

### 1.1 Overview

Recently, the silicon-based materials and structures that emit light with a high quantum efficiency have been investigated to reply the desire for the integration of optoelectronic devices with silicon microelectronics. In silicon science and technology, crystalline silicon is the outstanding material in microelectronics and is studied widely. It does not show efficient light emission at room temperature because its band structure possesses an indirect gap of about 1.1 eV. One promising approach to overcome the indirect nature of optical transition in crystalline silicon is the relaxation of  $k$ -selection rule due to the spatial confinement in low-dimensional silicon nanostructures. Typically, in low-dimensional semiconductor systems, three kinds are determined : two-dimensional (2D) quantum wells, one-dimensional (1D) quantum wires, and zero-dimensional (0D) quantum dots. Silicon nanometer-size crystallites on 0D systems show the efficient visible light emission even at room temperature (Kenemitsu, Kondo and Takeda, 1994). The discovery of luminescence from nanometer-size crystallites is an extremely important scientific breakthrough. It leads to enormous technological implications because it initiates a new possibility for group-IV indirect-gap semiconductors as materials for optoelectronic applications (Kenemitsu et al., 1994; Zeng and Tsu, 1994; Lockwood,1994).

Porous silicon, one type of nanometer-size crystallites (nanocrystal), is widely interesting recently. However, it is not a new material. Fifty years ago, it

was first made by the Uhlir (1956) at Bell labs, USA during studies of the electropolishing of crystalline silicon in hydrofluoric acid based solutions. However, within 35 years before 1990, less than 200 papers relating to porous silicon were published. Most studies concern only its microstructure and general properties.

Currently, more widely interests in porous silicon resulted from the proposal (Canham, 1990), in 1990, concerning the efficient visible light emission from high porosity structures arises from quantum confinement effects. Particularly, this is surprising for three reasons. First, because porous silicon is composed of silicon structure and bulk silicon is inefficient to emit light, certainly, even at cryogenic temperature. Second, because the light emitting nanostructure can be easily carried out within minutes, without using both the costly lithographic and epitaxial techniques, the conventional approaches to realize exceeding small structures that practically available at that time. Third, because silicon is the most widely known technologically important material, leading to the microelectronics revolution that effect our everyday lives. Light-emitting silicon devices could result in a new generation of silicon chips and extend the functionality of silicon technology from microelectronics to optoelectronics. Comprehensive reviews about porous silicon are established such as that of Cullis, Canham and Calcott (1997), John and Singh (1995) and Smith and Collins (1992).

Before going on to our work, to introduce the porous silicon basically, we shall briefly elaborate about porous silicon in various aspects i.e. fabrication, structure, some optical and electrical properties, as well as theoretical studies.

## 1.2 Fabrication of Porous Silicon

### 1.2.1 Formation Mechanism

Various models have been proposed to try to explain the various structure of porous silicon forming in hydrofluoric acid-based solutions and were the point of a comprehensive review by Smith and Collins (1992). Various models have been put forward to clarify the formation of porous structures, however, it is largely agreed that the etching reaction requires holes injected from crystalline silicon substrate. A model for porous silicon formation suggested by Lehmann, Jobst, Muschik et al. (1993) is roughly described here. Figure 1.1 illustrates the diagram of porous silicon fabrication cell and the particular procedures involved in anodic etching at and close to the pore. It relies on the fact that holes are needed in the electrochemical dissolution process of silicon. Because of the increment of band gap in porous silicon compared with that of bulk crystalline silicon due to the quantum confinement effect, the additional energy  $E_q$  is necessary for holes in order to penetrate into the porous layer (lower right sketch in Figure 1.1). If  $E_q$  is larger than the bias, the holes are depleted and dissolution is not further. Since  $E_q$  is a function of the size of nanocrystallites, it can be concluded that an increment of the formation of bias causes an increment of the band gap energy and a decrement of the crystallite size in the porous layer. This process is self-adjusting and the size of the nanocrystallites is limited by the quantum confinement effect (Lehmann et al., 1993).

We here refer to related work and particularly intensity developments. Whilst, many models pay attention to how the pores propagate (Smith and Collins, 1992), just a few works explain why the first nucleates on the surface. The recent Kang-Jorre model (Kang and Jorre, 1993) mathematically treats pore

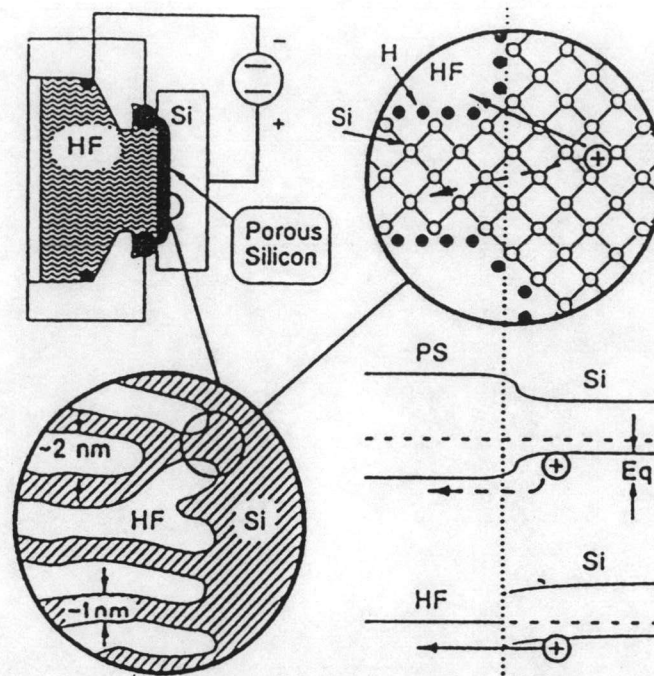


Figure 1.1: Schematics of porous silicon fabrication (upper left), the chemical process in anodic etching near the pore (lower left and upper right), and the band diagram for silicon-electrolyte transition at the pore and between the bulk and porous silicon (lower right) (Lehmann et al., 1993)

nucleation as the instability of a planar surface to small perturbations. Corbett, Shereshevskii and Verner (1995) have advised that near-surface vacancy supersaturation results in pore nucleation. Allongue, Devilleneuve, Pinsard et al. (1995) have intimated that hydrogen supersaturation produces micro-defects which are thence selectively etched. Experimental examination of point defect distributions at the first place of porous layer formation and below porous layers may distribute considerable understanding.

In addition, a few experimental studies aimed at pore nucleation kinetics, for example, the steadily increasing of surface pore density during an anneal period and the existence of an induction time prior to pore nucleation (Guilenger, Kelly, Chason et al., 1995). Number of further study is required in this area.

### 1.2.2 Anodization

Various luminescent porous silicon films fabricating methods, i.e., stain etching, have been briefly described in a few reviews (Jung, Shih and Kwong, 1993; Halimaoui, 1995). However, these methods are not described in any detail here. We shall stress on the anodization method.

Typically, anodization under galvanostatic conditions is the preferred choice for gaining wide ranges of porosity and thickness reproducibly. Neatly preparation of the electrochemical cell is essential in order to attain good lateral film uniformity, as discussed by Halimaoui (1995). Layer microstructure is sensitive to many parameters which need to be controlled carefully during etching. These include electrolyte composition, current density, applied potential as well as electrolyte temperature if excellent reproducibility is to be achieved.

Ethanol is usually added to the hydrofluoric acid to minimize hydrogen bubble formation during anodization and accordingly improve uniformity of the layer. Luminescent porous silicon layers fabricated in both dilute aqueous hydrofluoric acid and ethanoic hydrofluoric acid are generally mesoporous, while the ones fabricated in concentrated (40-50wt%) aqueous hydrofluoric acid can be entirely microporous.

## 1.3 Structure of Porous Silicon

A porous, brittle silicon skeleton exhibiting a variety of pore geometries is obtained. The controlling parameters in the anodization process are the dopant concentration in the silicon substrate, the dopant type (n or p), the current density and the electrolyte concentration. The observed morphologies vary from a

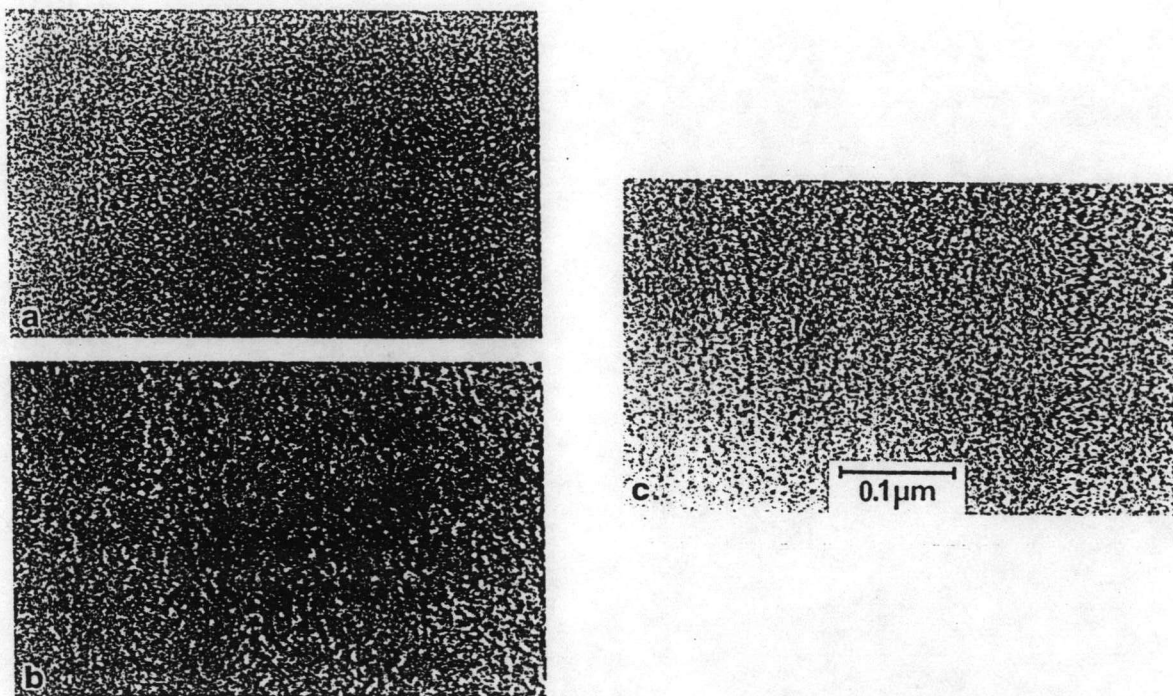


Figure 1.2: TEM cross-sectional images of a porous silicon structure formed by anodizing  $p^-$  silicon : (a) 36% porosity, (b) 52% porosity and (c) 64% porosity (Beale et al., 1985)

uniform network of fine interconnected pores to linear and wide pipe-like pores. Figure 1.2 shows TEM cross-sectional images of a porous silicon.

TEM micrographs of porous silicon have been reported by several workers (Smith and Collins, 1992; Beale, Benjamin, Uren et al., 1985). they reveal that porous silicon consists of isolated crystallites and/or chains of crystallites linked by narrow silicon walls. An important aspect is that the silicon in the crystallites retains its bulk-like character. The nature of the pore geometries formed depends on the controlling parameters. A p-type silicon substrate forms a uniform and highly interconnected network of random pores, resulting in a spongy structure. In n-type, the pores are formed only under illumination and are relatively linear. For degenerately doped cases (both  $p^+$  and  $n^+$ ), the geometries are similar to the interconnected p-type structure, but with shorter and wider pores. At higher

Type of porous silicon	Corresponding size regime for dominant porosity (nm)
Microporous	$\leq 2$
Mesoporous	2 - 50
Macroporous	$> 50$

Table 1.1: Pore size classification (Cullis, Canham, and Calcott, 1997)

current densities, the pores widen further. In n-type, the linear pores tend to become pipe like in this case. At very high currents, silicon is uniformly etched away leading to electropolishing. This can also occur at very low hydrofluoric acid concentration.

The most common characterization parameter employed to describe the porous silicon morphologies is the sample porosity. Assuming a silicon wafer is completely connected to porous silicon, the porosity  $p$  is calculated as (John and Singh, 1995)

$$p = \frac{\text{mass of silicon wafer} - \text{mass of porous silicon film}}{\text{mass of porous silicon film}} \times 100. \quad (1.1)$$

Sample having porosity  $> 60\%$  are found to luminesce in the visible region.

Generally, porous media should also be classified on the basis of the IUPAC guidelines (Rouquerol, Avnir, Fairbridge et al., 1994) which define ranges of pore size showing characteristic absorption properties (Table 1.1). The literature relating to porous silicon seldom uses the term "microporous" and exhibits no similarity to the strict criteria now accepted universally by workers studying porous carbons, glasses, etc. Certainly, it will be clear that part of the problem is that the optoelectronic properties of porous silicon are largely determined

Spectral range	Peak wavelength (nm)	Luminescence band label	Photo-luminescence	Electro-luminescence
UV	~350	UV band	Yes	No
Blue-green	~470	F-band	Yes	No
Blue-red	400-800	S-band	Yes	Yes
Near IR	1100-1500	IR-band	Yes	No

Table 1.2: Porous silicon luminescence bands (Cullis, Canham, and Calcott, 1997)

by skeleton size not pore size. Nevertheless, the form of porosity still largely determines many properties relevant to characterization and material processing. Semiconductor-inspired new terminology such as "nanoporous" is currently poorly defined but has been invoked, presumably, to indicate a solid skeleton with dimensions small enough to form a nanostructure.

## 1.4 Some Properties of Porous Silicon

### 1.4.1 Photoluminescence

Porous silicon based structures have been presented to efficiently luminescence across the whole range from the near infrared through the visible region and into the near ultraviolet. Such broad range emission generates from a small number of clearly distinct luminescence bands of different origin, which are listed in Table 1.2.

In general, properties of each luminescence band and conditions under which they are created have been mentioned briefly in a number of reports (Canham, 1995). So far, "S-band" luminescence has been known as the most attentive



and the most technologically significant since it can be efficiently electrically excited. This band has been tuned through the visible range from deep red to blue (Mizuno, Koyama and Koshida, 1996).

The blue-green photoluminescence emission was first reported by Harvey et al. in 1992, who present rather strong blue-green photoluminescence output from oxidized porous silicon prepared by rapid thermal oxidation treatment. It is called "F-band" because of its fast nanosecond decay time. Several studies (Canham, 1995; Tsybeskov, Vandyshev and Fauchet, 1994; Harris, Syvajarvi, Bergman et al., 1994; Kux, Kovalev and Koch, 1995; Kux, Kovalev and Koch, 1995) have also subjected to this band. But it is observed only in oxidized structure and is very possible to arise from contaminated (Canham, Loni, Calcott et al., 1996) or defective silicon oxide (Tsybeskov et al., 1994).

Fauchet, Ettetdgui, Raisanen et al. (1993) have first found infrared emission at room temperature for material annealed under ultrahigh vacuum. It is discussed that this radiation origin could be dangling bond related (Mauckner, Hamann, Rebitzer et al., 1995) although no direct consistent result has been assured.

The other emission which was first reported by Jiang, Coulthard, Sham et al. (1993) is ultraviolet emission. It was found in 1993 from oxidized material under soft x-ray excitation. Consequently, the stronger output at room temperature has been proposed (Zuk, Kuduk, Kulik et al., 1993; Lin, Yao, Duan et al., 1996; Qin, Lin, Duan et al., 1996; Chen, Zhou, Zhu et al., 1996). As same as the blue-green F-band, the UV bands are observed only from oxidized layers and also are likely to created from the defective oxide phase (Lin et al., 1996).

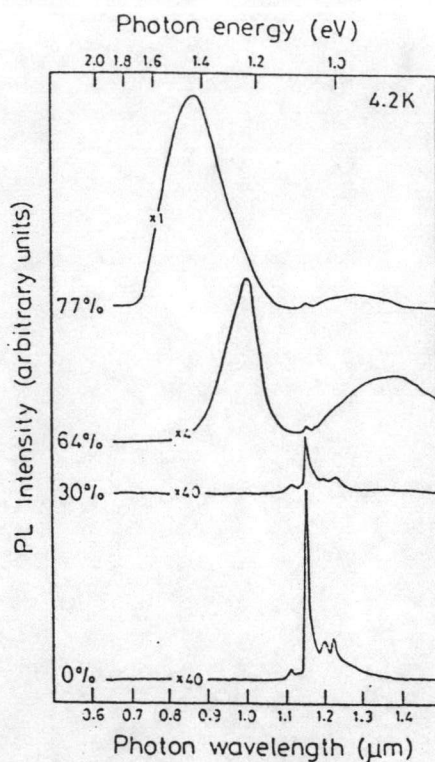


Figure 1.3: Low temperature photoluminescence of freshly etched layers of widely varying porosity: 0%-77%.

#### 1.4.1.1 Trends with Porosity

Figure 1.3 illustrates the porosity dependence of photoluminescence, increasing porosity resulting in stronger photoluminescent. The relative strengths of light output from the low and high porosity silicon layers can be compared with that of the underlying bulk substrate by photoluminescence spectroscopy at low temperature (4.2K). It is significant to note that the photoluminescence of 30% porosity layer cannot be detected. Indeed, it was noted that the S-band photoluminescence efficiency was not proportional to the internal surface area of the material, at an early stage, but that some "threshold" porosity had to be exceeded prior to efficient luminescence being detected. More than one photoluminescence band can be observed in high porosity layers but it is the porous silicon S-band that shifts into the visible region and becomes highly efficient. Figure 1.4 illustrates

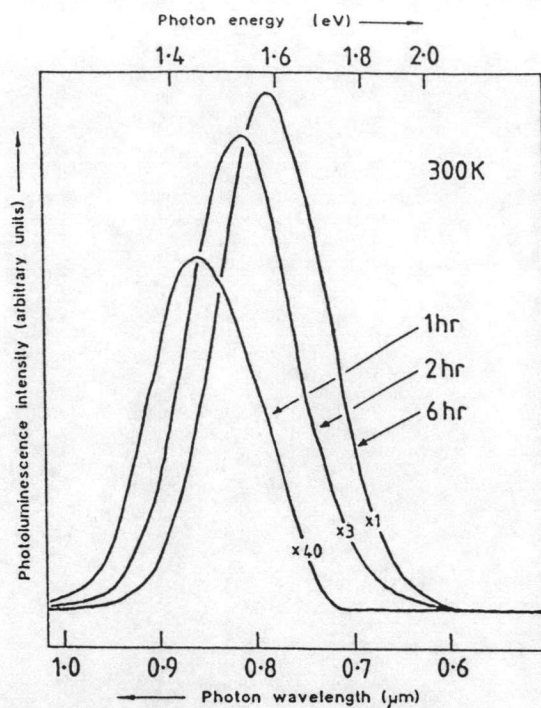


Figure 1.4: Room temperature photoluminescence of a freshly etched layer as a result of partial chemical dissolution in 40% aqueous hydrofluoric acid for the times indicated (Canham, 1990)

such spectra which was published the first (Canham, 1990). It shows a typical trend of different layers prepared by anodization with a variation of two parameters which are current density and anodization time. This figure shows the typical trend of a single layer which is continuously chemically etched, post-anodization (Canham, 1990). A significant increment in photoluminescence output together with an observed blue shift of photoluminescence peak position is shown while the porosity is rising. This is confirmed by gravimetric method which detects an amount of silicon removed from the structure. Because the removal of silicon makes an overall decrease in silicon skeleton size, in 1990 strong indirect evidence for quantum size effects was established.

Efficient visible photoluminescence can be obtained from high porosity homogeneous layers in anodized substrates of all types ( $n^-$ ,  $p^-$ ,  $n^+$ ,  $p^+$ ). However, the efficiencies regularly decrease in that order.

For "just finished" etched material, high porosity is constantly occurred and then results in high photoluminescence efficiency. This is contrast to isolated early reports which suggest that material of low porosity, even at 10% porosity, can be luminescent visibly. Inefficient visible photoluminescence can be occurred in inhomogeneous material of low average porosity, but the light still can be emitted from microscopic high porosity area. The typical example is the macroporous material fabricated from  $n^-$  wafers in which each macropore is actually lined with luminescent mesoporous material.

### 1.4.2 Electroluminescence and Devices

A photoluminescent material can possess efficient electrically excited luminescence, if it is treated by some methods. Both injection and transportation of excited carriers of both types through the luminescent material with minimized energy loss, due to nonradiative processes, are the examples. However, it is uncertain if efficient electroluminescence will be occurred. So, giving of some insight indirectly into both luminescent mechanism related and into the structure of the luminescent material is required (e.g., structural connectivity in the case of porous materials).

So far, there have been continuous studies of electroluminescent porous silicon based diodes (Koshida, and Koyama, 1992; Steiner, Kozlowski and Lang, 1993; Linnros and Lalic, 1995; Loni, Simons, Cox et al., 1995). The early reports are those of Koshida and Koyama (1992). Figure 1.5 illustrates a schematic of the first Koshida LED and its electroluminescence spectral output (Koshida and Koyama, 1992). Typically, the many primary works apply a device structure

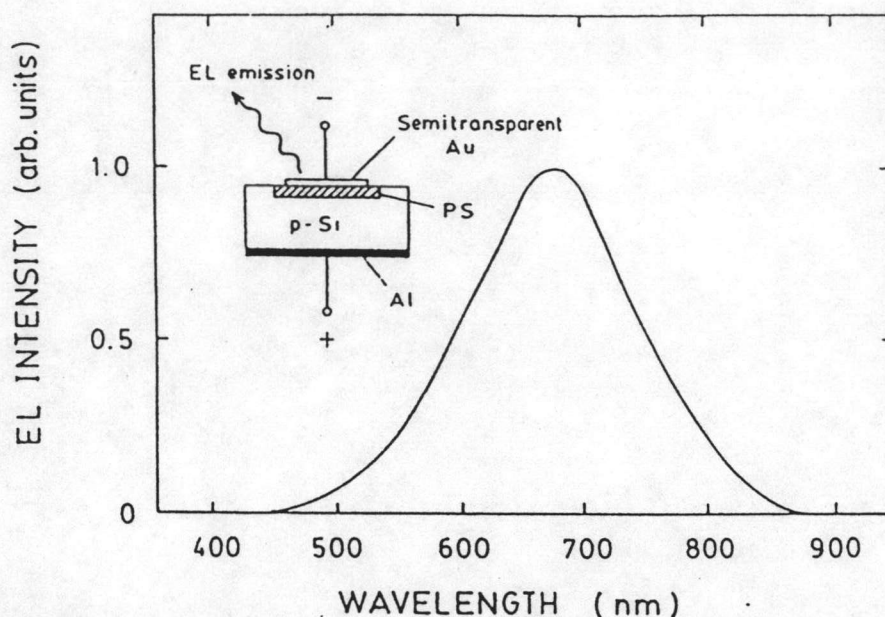


Figure 1.5: Schematic diagram of one of the first porous silicon LEDs with its visible electroluminescence spectrum (Koshida and Koyama, 1992)

of a semi-transparent contact layer deposited on top of a freshly etched photoluminescence porous silicon layer. This first prototype device has an external quantum efficiency (EQE) for electroluminescence of only  $10^{-5}\%$ , some five orders of magnitude lower than the likely photoluminescent efficiency of the same layer.

A number of reviews (Wang, Wilson and Haegel, 1993; Martinez-Duart,

Electrical contact	Type of substrate/porosity	Electrical threshold		(%EQE)
		(V)	(mA cm <sup>-2</sup> )	
Au	n <sup>-</sup> (meso)	~5	~50	10 <sup>-5</sup>
Au	p <sup>+</sup> n <sup>-</sup> (meso-macro)	~5	~0.1	10 <sup>-2</sup>
ITO	p <sup>+</sup> n <sup>-</sup> (micro)	~2.3	~0.001	0.2
Al/poly Si	n <sup>+</sup> p <sup>-</sup> (meso)	~2	~1.0	< 0.1
Al	n <sup>+</sup> (meso)	~6	-	10 <sup>-2</sup>

Table 1.3: Porous silicon LED characteristics (Cullis, Canham, and Calcott, 1997)

Parkhutik, Guerrero-Lemus et al., 1995; Canham, Cox, Loni et al., 1996) briefly discuss the worldwide development of electroluminescent efficiency which lead to multicolored electroluminescence, etc., such as that of Fathauer, George, Ksendzov et al. (1992) Table 1.3 exhibits various structure and performance of selected porous silicon LED's.

In 1993, an anodized  $p^+ n^-$  silicon diode structure composed of both mesoporous and macroporous regions was suggested to contribute an EQE of approximately  $10^{-2}\%$ . Later on, it has been shown that this device exhibits a high EQE of 0.16%, under relatively high bias (20V), although only a low power efficiency of  $10^{-4}\%$  is gained. Most recently, it has been exhibited that an improved silicon LED composed of only microporous material can be fabricated by ion implantation with carefully controlled processing to obtain an EQE of approaching 0.2%. The obtainable efficiency is now close to a practical useful level of 1%.

Furthermore, it is important to emphasize that a major affinity of porous silicon LEDs is that actually they are VLSI-compatible silicon devices. This recently exemplified by the work of Hirschman, Tsybeskov, Dutttagupta et al. (1996) relating to the integration of a porous silicon LED with standard bipolar circuitry. An another interesting recent research is the manipulation of microcavities to develop LED performance (Pavesi, Guardini and Mazzoleni, 1996). These structures have the capability to

- (a) convincingly reduce the spectral width of electroluminescent output,
- (b) improve the directionality of such output,
- (c) reduce the radiative decay time,
- (d) enhance the EQE if the electrical transport through such multilayer

structures is controlled well.

Moreover, Canham (1993) indicates that the range of electroluminescent tunability can be effected by vertical inhomogeneity within the layer. Consequently, Bsiesy, Muller, Ligeon et al. (1993) and Meulenkamp, Peter, Riley et al. (1995) also try to determine this issue by studying the effect in layers of varying thickness. They are disagree (Bsiesy et al., 1993) or at least implied (Meulenkamp et al., 1995) that the thinner layers have a substantially reduced porosity gradient and yet still exhibit electroluminescent tunability. Nevertheless, almost all luminescent layers, either thick or thin, compose of porosity gradient distinctly. So the effect of vertical inhomogeneity, if any, still cannot be solved.

However, it is generally accepted that the phenomenon has a natural explanation within a quantum confinement framework (Bsiesy, Muller, Ligeon et al. 1993; Canham, 1993; Bsiesy, Muller, Ligeon et al. 1994; Bsiesy, Gaspard, Herino et al, 1995; Ogasawara, Momma and Osaka, 1995; Mihalcescu, Vial, Bsiesy et al., 1995; Meulenkamp et al., 1995). At the present time, a model of Meulenkamp et al. (1995) is known as the most detail and successful. They consider tunability to generate from the switch-on and quenching processed. Both processes are voltage dependent due to size effects. In addition, they consider the kinetics of carrier injection within a whole luminescent particles by Gaussian size distribution and attribute quenching to the injection of an electron into a particle that already contains an exciton, therefore leading to non-radiative Auger recombination (Mihalcescu et al., 1995). By such a model, the experimental data can be simulated satisfactorily. It seems questionably that the many light emission models, which do not induce quantum confinement, can explain such a phenomenon.

And actually, no such explanations have been proposed.

### 1.4.3 Optical Absorption

Lehmann and Gösele (1991), who initiate the interest in the absorption in porous silicon, have made a comparison of optical transmission between bulk silicon and free standing porous silicon films fabricated from p and p<sup>+</sup> silicon. It manifests that the transmission below the direct gap is dramatically increased in the porous sample relative to the bulk silicon. Their reason leans on quantum confinement effects which cause the increasing of band gap of the porous silicon compared to bulk silicon (Lehmann and Gösele, 1991).

Consequently, various technique have been manipulated to investigate optical absorption in porous silicon including transmission measurements (Lehmann and Gösele, 1991; Grivickas and Basmaji, 1993; Ookubo, 1993; Ito, T., Ohta and Hiraki, 1992; Kenemitsu, 1994; Xie, Hybertsen, Wilson et al., 1994; Matsumoto, Daimon, Futagi et al., 1992; Owrutsky, Rice, Guha et al., 1995; Koch, Petrova-Koch and Muschik et al., 1993; Wang et al., 1993; Sagnes, Halimaoui, Vincent et al., 1993; Mauckner, Rebitzer, Thonke et al., 1994; Nomura, Zhao, Schoenfeld et al., 1994; Kovalev, Polisski, Ben-Chorin et al., 1996), photoluminescent excitation (Zhang, Lerner, Alekel et al., 1993; Ookubo, 1993; Xie, Wilson, Ross et al., 1992; Kenemitsu, Uto, Masumoto et al., 1993; Bondarenko, Dorofeev, Filippov et al., 1993; Matsumoto et al., 1992; Bala, Firszt, Nossarzewska-Orlowska et al., 1993; Stutzmann, Brandt, Rosenbauer et al., 1993; Kanemitsu, Matsumoto, Futagi et al., 1993; Zheng, Liu, Bao et al., 1993; Zheng, Yang, Yan et al., 1994; Sinha, Banerjee and Arora et al., 1994; Bondarenko, Borisenko, Dorofeev et al., 1994;



Ito, Motoi, Arakaki et al., 1994; Kux and Ben-Chorin 1995; Kux, Kovalev and Koch, 1995; Ito, Yoneda, Furuta et al., 1995), photothermal spectroscopy (Chan, So, Cheah et al., 1996; Yarkin, Konstantinova and Timoshenko, 1995) and spectroscopic ellipsometry (Canham, Cullis, Pickering et al., 1994; Pickering, Canham and Brumhead, 1993; Ferrieu, Halimaoui and Bensahel, 1992; Larre, Halimaoui, Glowacki et al., 1994). The results obtained from absorption measurements are difficult to comprehend because there are conditions on detail of experiment and also on issues of interpretation. Generally the difficulty of interpretation caused by the microscopic inhomogeneity in porous silicon. Certainly, all samples have a distribution of sizes of silicon structures, and subsequently the absorption at any wavelength will be a sum of widely differing microscopic absorption responses. Furthermore, comparison of absorption strength between this material and bulk silicon has to be particularly considered on the basis of its porous property, usually through the Bruggeman effective medium approximation.

The upshift of the absorption in the wavelength range between the indirect and direct gaps of bulk silicon has originally studied by Lehmann and Gösele (1991), and afterward Sanges et al. (1993) have followed in more detail. They have measured the transmission of free standing p and p<sup>+</sup> porous silicon samples with a variation of porosities. In this work, the errors of the derived values of absorption due to perpendicular or lateral sample inhomogeneity have been prevented carefully. Also, the effects of reflection and of the quantity of absorbing material have been definitely incorporated into the analysis.

In Figure 1.6, the square root of the absorption coefficient, multiplied by the photon energy,  $(\alpha\hbar\nu)^{1/2}$ , is plotted versus photon energy for bulk silicon and two p and p<sup>+</sup> porous silicon layers. For bulk silicon, linear relation between

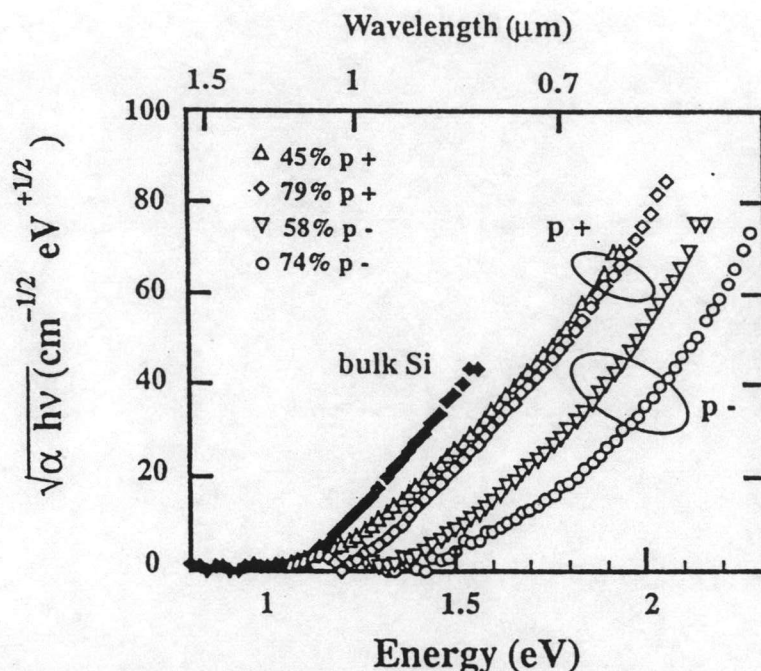


Figure 1.6: Square root of the absorption coefficient times photon energy vs photon energy for porous silicon p and p<sup>+</sup> layers (Sanges et al., 1993)

$(\alpha h\nu)^{1/2}$  and photon energy is illustrated, as is expected near the gap for an indirect gap semiconductor (Johnson, 1967). In case of p<sup>+</sup> layers such relation is almost linear and shows a porosity dependent shift to higher energy of up to 100 meV. For the p layers, the plots are obviously non-linear and show an energy upshift of between 300 and 500 meV relative to bulk silicon. The shifts are corresponding to porosity, higher porosity causes larger shift. The authors have concluded that this shift is due to a quantum size effect (Sanges et al., 1993). Consequently, it can be said that the smaller dimensions of the silicon structures in the p-type layers lead to the upshifted absorption of p porous silicon layers relative to p<sup>+</sup> porous silicon layers.

Other studies also accordingly reported similar absorption results and absorption upshifts. These include a study of Kovalev et al. (1996). Figure 1.7 illustrates a plot of  $\log(\alpha)$  versus photon energy for bulk crystalline silicon, amorphous silicon, microporous silicon and for calculations of the absorption in

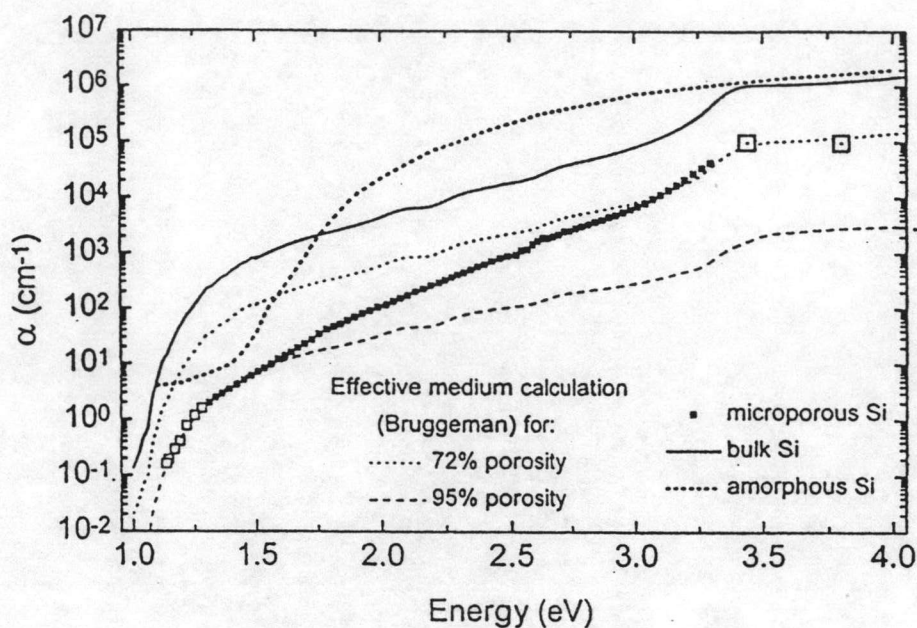


Figure 1.7: Spectral dependence of the absorption coefficient of free-standing microporous silicon (solid squares), bulk silicon (solid line) and amorphous silicon (heavy dotted line) at 300K. Effective medium calculations using the Bruggeman approximation for silicon spheres embedded in vacuum are also shown: the dotted line represents 72% porosity (the nominal porosity of the microporous silicon samples studied) the dashed line represents 95% porosity. Individual large open squares represent values of  $\alpha$  obtained with discrete lines of the argon laser. Smaller open squares represent data points considered to be less reliable (Kovalev et al., 1996)

porous silicon films of two different, 72% and 95%, porosity based on Bruggeman effective medium model with exclusion of confinement effects. Above the direct gap of bulk silicon, the experimental results overlie the Bruggeman results calculating for 72% porosity. Below the direct gap the absorption of the porous silicon is less than that of the Bruggeman model by an amount that increases with decreasing energy until close to the indirect gap. These results agree with those of the other transmission studies elucidated earlier. In this range of wavelength, the absorption coefficient of porous silicon exponentially depends on energy with a slope of approximately 180 meV. The absorption in bulk silicon is exponential in this region, as is the absorption in amorphous silicon below 1.8 eV in the Urbach tail (Cody, Tiedje, Abeles et al., 1981). The former proposal is the simple confinement model, the latter model assumes that the absorption is into disordered induced surface states which is presented at the large internal surface of porous silicon (Koshida and Koyama, 1992). In work of Kovalev et al. (1996), the authors have studied both models and the crystalline silicon model has found to be preferred. According to their investigation of the absorption at temperatures between 7 and 400K, it is shown that plots of  $\log(\alpha)$  versus energy for various temperature provide a series of parallel lines, with stronger absorption at higher temperature. This is contradicted to the Urbach tail-state model, which predicts that such plots should extrapolate to a common point (Wiley, Thomas, Schonherr et al., 1980). The crystalline model presumes that increased temperature should result in a downward shift of the band gap and an improvement of phonon-assisted absorption. Such effects agree with the observed results. Additionally, it has been found that desorbing hydrogen which result in increasing of surface disorder does not dramatically influence the absorption characteristics, in

disagreement with the predictions of the Urbach tail-state model (Kovalev et al., 1996).

It has been reported that besides the transmission, the others experimental techniques also play an important role in studying of the absorption because the conclusions of the work are primarily corresponding to the results of transmission measurements. Nevertheless, it has been noted that close to indirect gap of bulk silicon, absorption in porous silicon films detected by photoluminescence excitation is convincingly weaker than the absorption detected by transmission (Ookubo, 1993; Kux and Ben-Chorin, 1995). This contradiction has been partly caused by artefacts in the transmission measurements due to effects, for example scattering and errors in the normalization of the photoluminescence excitation measurements (Ookubo, 1993). However, these two effects may not be the major effects. Since photoluminescence excitation measures only absorption that leads to luminescence at a particular energy so the existence of absorbing non-luminescent material reduces the absorption measured by photoluminescence excitation compared to that of transmission. In fact, porous silicon does contain such material in the form of large (non-confining) particles (Binder, Edelmann, Metzger et al., 1996), so the effect of which will be most revealed near the indirect gap. At this point, the ratio of the absorption of the bulklike larger particle to the luminescent, confinement-upshifted material will be largest. Also, the presence of such bulklike material has been concluded from attentive analysis of transmission measurements near the indirect gap (Kovalev et al., 1996).

Recently, Datta and Narasimhan (1999) proposed a modelled for optical absorption in porous silicon. They model the absorption process by assumable considering porous silicon as a pseudo-one-dimensional material system which

possess a distribution of band gaps. They also indicate that in order to explain the absorption, we specifically need the following assumption to be involved

(a) the momentum is not conserved in optical transitions (non-phonon assisted transition),

(b) the oscillator strength of these transitions depends on the size of the nanostructure in which the absorption takes place,

(c) the distribution of band gaps significantly influences the optical absorption.

However, a number of suspects in this model still remains. The anisotropic of the model, which contrast with actual experimental result, is an example. Further suspect is the assumption of the presence of only one type process (phonon-assisted processes) which disputes the experimental result (Kovalev, Heckler, Ben-Chorin et al., 1998).

#### **1.4.4 Electrical Conduction Mechanism**

The next fundamental issue concerning light emitting porous silicon is apparently the transport mechanism. This mechanism is dramatically interesting because it obviously correlates to electroluminescence and subsequently to the practical application of this system. A number of suggestions, available at this present time, for the paths range from transport in the crystallites (Tsu and Babi, 1994), diffusion (Pavesi and Ceschini, 1993), or tunneling (Diligenti, Nannini, Pennelli et al., 1996) between the crystallites or on their surface (Diligenti et al., 1996; Mare, Kritofik, Pangrac et al., 1993). Transport in a disordered silicon tissue (e.g., hydrogenated amorphous silicon) which wraps the crystallites has been reported additionally (Koka, Pelant and Fejfar, 1996; Lubianiker, Balberg, Partee

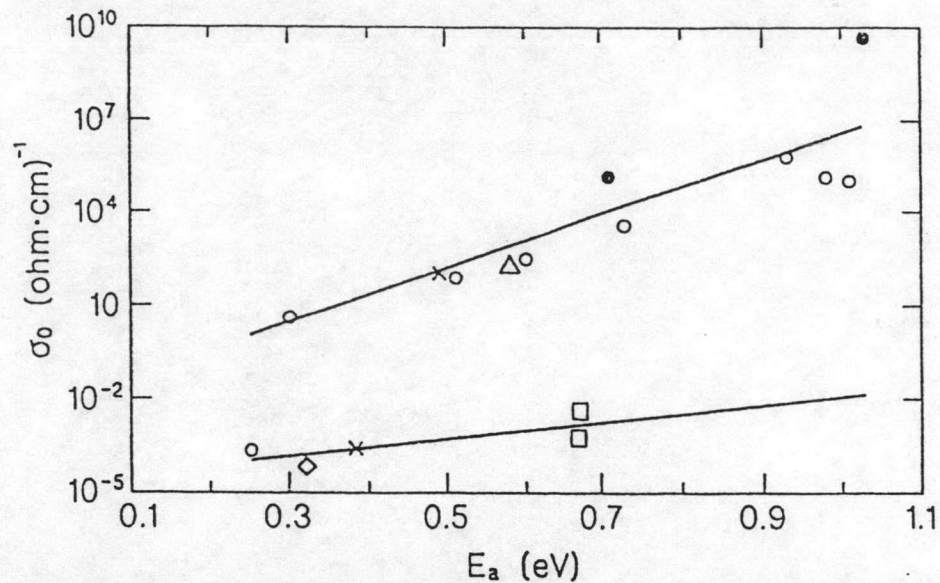


Figure 1.8: The experimentally determined values of the dc-conductivity prefactors as a function of the corresponding activation energies in a variety of porous silicon samples. The sources of the data are indicated in the figure. The solid lines represent the best fit to a MNR for transport in extended states (upper line), and for transport by activated hopping (lower line) (Lubianiker and Balberg, 1997).

et al., 1996). Various mechanisms have been put forward including band conduction (Koyama and Koshida 1993), activated hopping in the tails (Koka, Pelant and Fejfar, 1996), activated deep states hopping (Ben Chorin, Möller and Koch, 1993), a Pool-Frankel process (Ben-Chorin, Möller and Koch, 1994) and activated hopping in fractal network (Ben-Chorin, Möller and Koch, 1995).

So far, the most reliable conclusion is that of Lubianiker and Balberg (1997) which divides the rather large number of proposed paths and mechanisms into two different transport mechanisms. In principle, they analyze all available published conductivity data within the framework of the Meyer-Nedel rule (MNR) (Yelon, Movaghar and Branz, 1992; Boisvert, Lewis and Yelon, 1995). Figure 1.8 illustrates the dc-conductivity prefactors as a function of the according activation energies in various porous silicon samples. The noticeable separation of porous

silicon data points into two groups clearly assures the presence of only two different conduction mechanisms. One is associated with extended-state transport while another is associated with activated hopping.

## 1.5 Models of Light Emission

In the first published work (Canham, 1990), quantum confinement of carriers in crystalline silicon wires was proposed as the origin of the luminescence. This work reveals emission of strong visible light from porous silicon at room temperature. Subsequently, numerous models have been applied in order to explain this phenomenon alternatively. The beginning of the visible luminescence from porous silicon has been suggested in a number of relatively short reviews. Here, we concern a much more comprehensive and detailed overview of the experimental and theoretical evidences which have collected during the recent period. The various proposed models can be sorted into six groups as illustrated in Figure 1.9. In each case, the heading explains the nature of the material proposed as the origin of the luminescence.

Consequently, the five extrinsic model groups are briefly described and their reasons together with the evidence are summarized. The models are then evaluated and only results which are well understood and clear are attended particularly. Finally, the status of the quantum-confinement model is discussed and ability of this model to explain the wealth of results presently available is evaluated.



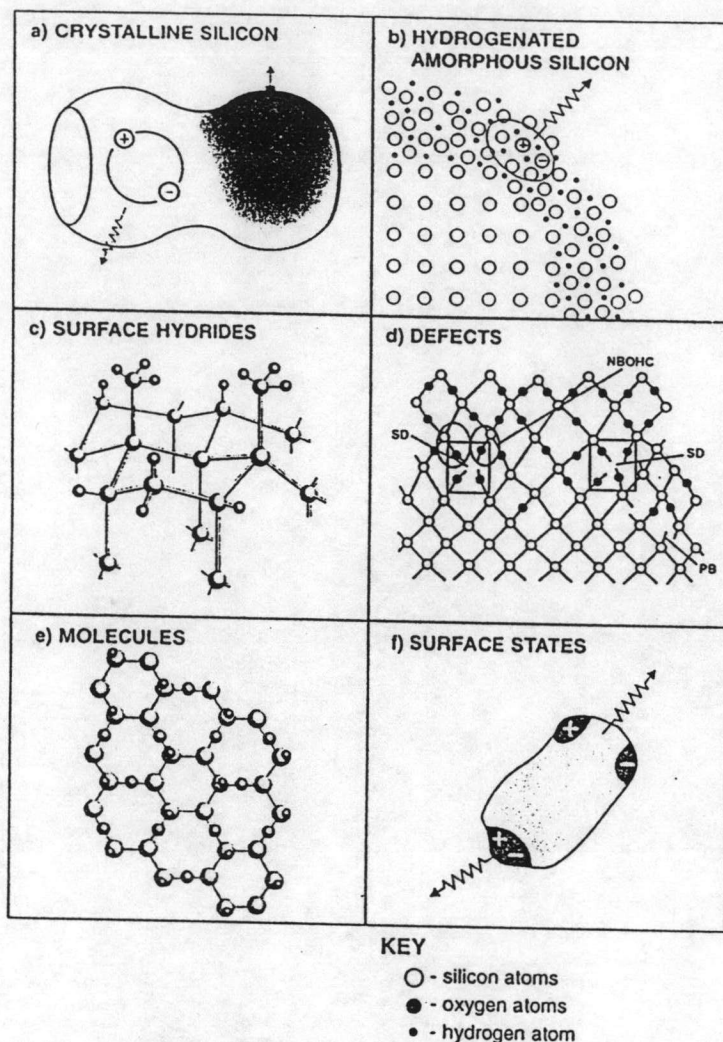


Figure 1.9: The six groups of models proposed to explain the photoluminescence from porous silicon. Detailed discussions of these various models are given in Section 1.5, here the model groups are illustrated pictorially under titles referring to the nature of luminescence material (Cullis, Canham and Calcott, 1997)

### 1.5.1 Hydrogenated Amorphous Silicon

In this model, the observed photoluminescence from porous silicon would come from a hydrogenated amorphous phase created by the anodizing process. It is known that hydrogenated amorphous originates a photoluminescence band (Vasquez, Madhukar and Tanguay, 1985) in the visible region. In addition, alloying effects that cause varying amounts of hydrogen and oxygen into the material could give a possible reason for the observed tunability of the photoluminescence from porous silicon. This model was increasingly interesting by early structural studies which reported significant amounts of amorphous material in luminescent porous silicon. More recently, some studies have still proposed that the luminescence is linked with highly disordered material (Estes and Moddel, 1996).

The weight of evidence is now undoubtedly opposed to the possibility that amorphous silicon causes the photoluminescence in porous silicon. TEM studies, where microscopic specimen damage in the preparation step have been minimized, have exhibited that there is little or no amorphous silicon in as form porous silicon specimen. In high porosity material, misorientation of nanocrystallites caused by ineluctable localized fragmentation of the silicon skeleton during drying is often evidenced, but the material is crystalline.

Moreover, there is an another strong negative evidence which is spectroscopic evidence that against the photoluminescence generating from an amorphous phase.

The intensification of photoluminescence as temperature increased from cryogenic value to 150K and the strong photoluminescence at room temperature is contrary to the photoluminescence observed in a-Si:H of which is strongly quenched as temperature increased.

In addition, the number, energies and relative strengths of the phonon replicas observed in resonantly excited photoluminescent spectra indicate that the luminescent material in porous silicon possess the electronic and vibrational band structure of crystalline silicon, and subsequently cannot be amorphous in nature.

### 1.5.2 Surface Hydrides

$\text{SiH}_2$  surface species were proposed to be the luminescent specie in porous silicon according to the observation that the photoluminescence intensely significantly decreases if the hydrogen is thermally desorbed from the anodized porous silicon surface. It is also deserved that the photoluminescence intensely can be regained with a brief hydrofluoric acid etch which restores the hydride coverage (Tsai, Li, Sarathy et al., 1991; Prokes, Glembocki, Bermudez et al., 1992).

This proposal followed the work which had indicated the existence of a tunable visible photoluminescence band proposed as caused by  $\text{SiH}_x$  groups (Wolford, Scott, Reimer et al., 1983).

Subsequently, the hydrogen desorption work has been redetermined and reinterpreted. Fourier transform infrared spectroscopy (FTIR) studies has shown that the photoluminescence is quenched while most of the hydrogen still remains on the silicon surface (Robinson, Dillon and George, 1993). The loss of the photoluminescence intensity as the hydrogen is desorbed more depends on the formation of an efficient nonradiative channel, through the creation of dangling bonds on the now poorly passivated surface of the silicon, than on the loss of a luminescent hydride species. Probably the most definitive evidence that surface

hydrides do not lead to the photoluminescence is the observation that efficient photoluminescence can also be produced from porous silicon where the hydride passivation has been replaced by a high quality oxide formed chemically or thermally. Thus, it is clear that hydride passivated porous silicon is only one of a number of possible luminescent forms of this material.

In addition, the observation of porous silicon samples with different morphologies shows no correlation of the photoluminescence intensity with hydride coverage. Macroporous silicon can have a large hydride passivated internal surface and yet shows no visible photoluminescence.

In fact, the work has demonstrated that the intensity of the photoluminescence from low porosity films can be heightened by over three orders of magnitude by an anodic oxidation that reduces the dimensions of the silicon material while reducing the hydrogen coverage, at the same time. Furthermore, the spectroscopic discussion previously strongly disputes against hydride surface species as the origin of the photoluminescence.

### 1.5.3 Molecules

Luminescent molecules occurred during the production of porous silicon, and then present on its surface, have been proposed as the origin of the efficient photoluminescence in this material (Xu, Gal and Gross, 1992).

Siloxene which is a Si/H/O-based polymer, particularly, has been proposed as a possible luminescent agent according to its general optical properties which resemble those of luminescent porous silicon (Brandt, Fuchs, Stutzmann et al., 1992). The photoluminescence spectrum of siloxene annealed at 400°C

and that of porous silicon are in the same region. Moreover, both IR absorption spectrum of annealed siloxene and that of aged porous silicon show same Si-Si, Si-O and Si-H vibration bands.

However, FTIR method applied on luminescent porous silicon, of which atmospheric oxidation is avoid, have shown no detectable oxygen in the material (Tischler and Collins, 1992; Dubin, Ozanam and Chazalviel, 1994). This result causes severe problems for molecules models for the origin of the photoluminescence in general, and the siloxene model in particular. In addition, it has been shown that oxide passivated porous silicon still be able to luminesce after thermal treatment at above 1000°C. Siloxene and other molecules would be decomposed completely at temperature below this. The spectroscopic result obtained from resonantly excited photoluminescence measurements also strongly debates against a molecule origin for the photoluminescence.

#### 1.5.4 Defects

This model explains the photoluminescence generated from porous silicon that the luminescence originates from carriers localized at extrinsic centers, both in the silicon and in an oxide that covers the silicon surface (Kenemitsu, Uto, Masumoto et al., 1993; Wang, Perz, Gaspari et al., 1993; Prokes, 1993). The evidence that efficient visible photoluminescence can be generated from nanocrystalline silicon nucleated in a variety of ways and passivated with hydrogen or oxygen disputes against the photoluminescence being due to an impurity specific defect center. It is also undoubted that models which rely on defects in an oxide layer cannot explain the photoluminescence from oxide-free "just finished" anodized porous

silicon. The large up-shift in the luminescence energy which is found among identical samples that is subjected to varying degrees of leaching in hydrofluoric acid, the tunability of the photoluminescence, also shows more impossibility of the defect models. This is because the energy levels of such defects should be mostly effected by the size of the silicon structure that they exist in. The spectroscopic evidence is also against defects as the origin of the photoluminescence. Particularly, the evidence from resonantly excited photoluminescence disagrees with carrier localization on an atomic scale at a defect site.

### 1.5.5 Surface States

Porous silicon contains very large internal surface. Such surface is proposed to be related to the emission process. In surface states model, absorption occurs in the quantum confined silicon but the radiative recombination happens in states localized at the surface of porous silicon or in a interfacial region between the silicon and an oxide. Deep surface states that strongly localize carriers (Koch, Petrova-Koch, Muschik et al., 1993) have been proposed and so, more recently, shallow surface states that do not strongly localize carriers (Koch, 1995) have introduced. The large energy difference between the absorption and photoluminescence peaks in porous silicon has been proposed as evidence that photocreated carriers relax into surface states.

Spectroscopic evidence is against that photoluminescence of porous silicon arised from deep surface states. The resonantly excited photoluminescence results (Cullis, Canham and Calcott, 1997) clearly show that the photoluminescence from porous silicon created from excitons which couple to momentum-conserving

phonons with momentum equal to the conduction band minimum of crystalline silicon. It is presumed that the wave function of the exciton is spread over many silicon atoms and is not localized on an atomic scale as found in the case of excitons localized at deep surface states.

If such a strong localization happened, momentum conservation would be totally cancelled and excitons would couple to phonons with a broad range of momenta. In addition, the excitons would also couple to phonons associated with local vibrational modes of the trapping center. The size of the exchange splitting in porous silicon given from resonantly excited photoluminescence spectra and extracted from temperature dependent lifetime measurements also indicates that carriers are not localized on atomic length scales, but rather sample the whole volume of the silicon nanostructures they exist in.

As referred to earlier, shallow surface states that only weakly localize carriers at the surface of crystalline silicon nanostructure also have been put forward (Tsai et al., 1991). The properties of such shallower surface states closely approach to those of pure bulk like states as the degree of surface localization reduces and this model is then closed to the quantum confinement model.

The present available spectroscopic evidences have not been enough to distinguish on this fine scale. Further theoretical and experimental studies are required in order to possibly determine the degree of surface localization of carriers in porous silicon.

### **1.5.6 Crystalline Silicon**

As mentioned earlier, the first model proposed to explain the efficient room temperature photoluminescence observed from porous silicon is quantum confine-

ment in crystalline silicon. In this model, quantum confinement effects widen the band gap of nanometer sized silicon structures and then leads to visible luminescence. Subsequently, the tunability of the photoluminescence when this material is leached in hydrofluoric acid can be explained by the size dependence of this upshift. In fresh structures, confinement is in wires of undulating width (Cullis and Canham, 1991) while in oxidized structures the geometry can be more dotlike (Bsiesy, Vial, Gaspard et al., 1991).

Because of the initial determination of light emission from porous silicon, many experimental and theoretical evidences have been now generated and such evidences strongly agree with the quantum confinement model, particularly these following substantial results.

Structural investigation has indicated that porous silicon is basically crystalline and also has estimated its dimensions of the nanostructures. Electronic structure calculations have qualitatively shown that the upshift of the photoluminescence found in porous silicon is according to that expected from silicon structure of the sizes observed and the upshift of the band gap in the silicon nanostructures have been observed in the absorption studies.

The observed decay times and calculated radiative lifetimes in model silicon wires and dots are qualitatively agreed. Also, the splitting of the lowest lying exciton states observed in the experiment has been able to be naturally explained by quantum confinement effects in silicon nanostructures. The strong spectroscopic evidence, in addition, assures the quantum confinement model. Resonantly excited photoluminescence spectra unclearly demonstrate that the luminescent material in porous silicon possess the electronic and vibrational band structure of crystalline silicon. Consequently, the quantum confinement model provides the



only explanation of porous silicon manner which is satisfactorily compatible with the main body of experimental and theoretical results now at hand.

However, at the present, there are a number of interesting observations which still require comprehensive explanation within the framework of quantum confinement effects. An example of such observations is the change in surface passivation that can induce wavelength shifts (Mihalcescu, Ligeon, Muller et al., 1993). The other example is the significant photochemical effects worked when layers are illuminated in hydrofluoric acid-based solutions (Létant and Vial, 1996). The last example is the structural effects which have to be examined when drying and rewetting porous silicon. Possibly, it seems that the partial collapse of the porous silicon network, due to liquid surface tension forces, can effect the quantum confinement behavior, while these processes might be reversible partly. Further studies are needed for aforementioned examples of the observations.

Notwithstanding, the shift due to a change in surface passivation, replacing of hydrogen by oxygen, is recently investigated and found to be success in order to explain the shift related to the trapping of an exciton by S=O bonds which produce localized levels in the band gap of nanocrystals that are smaller than  $\sim 3$  nm (Wolkin, Jorne, Fauchet et al., 1999). Thus, the explanations within the quantum confinement model just possibly seem to be approaching if all relevant factors have been entirely covered.

## 1.6 Theoretical calculation of optical properties

### 1.6.1 Model Structures and Calculation Techniques

The effects of quantum confinement on the electronic properties of silicon play an important role due to the structural observation that luminescent porous silicon contains crystalline silicon structures on a nanometer scale. Primarily, calculations have been done on idealized silicon wire and dot structures. Band structure have been performed using semi-empirical (Sanders and Chang, 1992; Proot, Delerue and Allan, 1992) and first-principles (Read, Needs, Nash et al., 1992; Buda, Kohanoff and Parrinello 1992; Ohno et al., 1992; Dorigoni, Bisi, Bernardini et al., 1996) calculations. Semi-empirical calculations have largely applied the tight binding approach. This approach employs a linear combination of atomic orbitals parameterized by fitting to the electronic band structure of bulk silicon at high symmetry point and, consequently, including adjustable parameters.

The tight binding approach is less calculatedly concentrated than first-principles calculations and therefore can deal with larger structure. Nevertheless the results of the tight binding approach applied to varying geometries and small dimensions are less reliable than the results of a first-principles approach because of the assumed transfer ability of bulk parameters inherent in. First-principle calculation are done on the basis of density function theory within the local density approximation (Hohenberg and Kohn, 1964; Kohn and Sham, 1965). The silicon core electrons are determined to remain in their atomic configurations and the interaction among the valence electrons, this core and the nucleus are demonstrated by a pseudo-potential. The obtained single particle orbitals are expanded in terms of a plane wave basis which is truncated in energy. The local density approximation approach has been discussed to be significantly successful

applying with the ground state properties of silicon, for example the total valence energy, providing results that are accurate to 1% (Jones and Gunnarsson, 1989). However, calculations of excited state properties are less accurate. In particular, a well known fault of the local density approximation approach is that the bulk silicon band gap is underestimated by approximately 0.6 eV caused by an inadequate treatment of the electron self-energy (Jones and Gunnarsson, 1989). Fortunately, this underestimate substantially independent on particle size, and accurate band gaps can be recovered for structures from the bulk to polysilanes by the simple accession of this constant correction (Delley and Steigmeier, 1995). A number of theoretical calculations are presented in a comprehensive review of John and Singh (1995).

Several wire and dot calculations suggest that the band gap in the confined structures is direct or pseudodirect. This clearly explains that dipole allowed transition can occurred without phonons participating in such structures. Nevertheless, for wide wires or large dots, bulklike phonon-assisted transitions is dominant since the strength of the dipole allowed transitions is weak. It is probably, in fact, not a matter to relate to the effects of confinement in terms of a direct or an indirect band cause the band structure description from which such terms derived is strictly valid only in the case of the actual translational symmetry of a bulk crystal or a perfect wire and invalid in irregular confined structures. Instead, a more practical approach is considered to discuss the effect of confinement in terms of the balance between non-phonon or momentum-conserving phonon-assisted radiative transitions (Hybertsen, 1994; Kovalev et al., 1998).

## 1.7 Our Work

As mentioned earlier, it appears that most calculations particularly assume porous silicon structure as an idealized structures (wires and/or dots) which are not disordered, perfect and not porous. Gösele and Lehmann (1992), based on their absorption experiment, have reported that porous silicon composed of an interconnected silicon skeleton which implies irregularity of the structure. Therefore, porous silicon is considered as a disordered material.

Here, the electronic structure of porous silicon based on disordered structure is first examined in this work. A primitive structure, the same as that of Sawada, Hamada and Ookubo (1994), is used in our work. Such structure is an irregular structure of porous silicon formed by removing some silicon atoms randomly from a perfect silicon crystal together with assuming that most dangling bonds of silicon atoms are terminated by hydrogen atoms. Here, some original symmetries definitely still remain in this structure, corresponding to the experimental evidence (Barla, Herino, Bomchil et al., 1984; Sugiyama and Nittono, 1990). In a sense, porous silicon can be considered as a disordered gathering of three dimension quantum wells which are yielded from random potential fluctuation from the system.

It is apparent that, in our model, the quantum confinement is implied throughout the potential fluctuation. This structure leads to decrement of density of states in the surrounding of the crystalline silicon band edges, similar to size effect in crystalline silicon model (Section 1.5.6), and to the localization of the electrons (or holes) near band edge. The reduction of density of states can obviously be observed from analytical approximated density of states which is achieved in our model by using Feynman's path-integral method for disordered

system (Sa-yakanit, 1979).

In addition, though the crystalline silicon model is widely accepted in order to explain the light emission arised from porous silicon, it still not be able to clearly explain the optical absorption. For the photoluminescence of porous silicon, the non-phonon assisted transition plays an important role while it shows no relation to the optical absorption. In case of optical absorption, porous silicon behaves like an indirect gap semiconductor (Kovalev et al., 1996), which its transition is phonon-assisted type.

To examine this suspect, the obtained density of states is applied to a simple model of absorption in order to calculate optical absorption coefficients, leading us to determine the energy range which significantly correlates with non-phonon process, as well as order of magnitude of the coefficients.

Furthermore, relying on Anderson's theory of localization (Anderson, 1958), the mobility gap clearly exists in our model. The localized states are separated from extended states by a mobility edge which relates directly to electrical conduction mechanism in porous silicon which cannot be explained by ordinary crystalline silicon model (Lubianiker and Balberg, 1997). Then not only optical properties but also electrical transport mechanism can reasonably be obtained from one model.

In this work, introduction about porous silicon is given in Chapter 1. The determination of density of states of porous silicon based on the above disordered model via Feynman's path-integral technique is available in Chapter 2 and the consequent mobility gap is roughly estimated as well. In Chapter 3, the density of states is applied to calculate the optical absorption coefficients in order to determine the energy range of absorption that significantly involve with non-

phonon assisted transition. Finally discussions and conclusions are described in Chapter 4.